Arabian Journal of Chemistry (2015) xxx, xxx–xxx

King Saud University

Arabian Journal of Chemistry

www.ksu.edu.sa
www.sciencedirect.com

ORIGINAL ARTICLE

Molecular modelling, synthesis, and antimalarial potentials of curcumin analogues containing heterocyclic ring

S.N. Balaji [a], Mohamed Jawed Ahsan [b,*], Surender Singh Jadav [c], Vishal Trivedi [a]

[a] *Malaria Research Group, Department of Biotechnology, Indian Institute of Technology-Guwahati, Guwahati 781039, Assam, India*
[b] *Department of Pharmaceutical Chemistry, Maharishi Arvind College of Pharmacy, Jaipur, Rajasthan 302039, India*
[c] *Department of Pharmaceutical Sciences & Technology, Birla Institute of Technology Mesra, Ranchi, Jharkhand 835 215, India*

Received 28 January 2015; accepted 12 April 2015

KEYWORDS

Antimalarial;
Curcumin analogues;
Kinase molecular modelling;
Plasmodium falciparum;
Pyrazole;
Pyrimidine

Abstract The molecular modelling approach was applied to a series of nineteen curcumin analogues to find the possible PfRIO2 kinase inhibitory action. A putative active site in flexible loop (S1) of PfRIO2 kinase was explored computationally to recognize the molecular basis of ligands binding. The ligands (curcumin analogues; **3a–3s**) were well accommodated in the selected active site (S1) due to their higher molecular size and length. Further all these synthesized compounds (**3a–3s**) were evaluated for their *in vitro* antimalarial activity according to the reported method. The antimalarial data showed that all these compounds to have parasiticidal activity with minimum killing concentrations (MKCs) range between 3.87 and 25.35 μM and schizonticidal activity with IC_{50} range between 1.48 and 23.09 μM. The compound **3p** showed the most significant result with maximum schizonticidal (IC_{50}; 1.48 ± 0.10 μM) and parasiticidal activities (MKC; 3.87 ± 0.36 μM) could be identified as promising lead for further investigations.

1. Introduction

Malaria is a life-threatening disease caused by five species of parasites and is transmitted through vector infected mosquito of genus *Anopheles*. An estimated 3.4 billion people are at risk of malaria and there are 107 countries and territories, where malaria is endemic. As per WHO report nearly 207 million cases of malaria and 627,000 death tolls occurred globally in 2012. Most of the cases and deaths occurred in unhygienic and developing African countries (WHO malaria report, 2013). Artemisinin combination therapy (ACTs) has been of much importance over the last decade however emergence of resistance has been reported in Cambodia's Pailin province (WHO malaria report, 2013; Phyo et al., 2012; Kumar et al., 2005) provides motivation to discover new potential antimalarial agents. More than 65 protein kinases (PKs) have been reported in the parasite kinome with ambiguous cellular target

* Corresponding author. Tel.: +91 9694087786; fax: +91 141 2335120.
E-mail address: jawedpharma@gmail.com (M.J. Ahsan).
Peer review under responsibility of King Saud University.

Production and hosting by Elsevier

http://dx.doi.org/10.1016/j.arabjc.2015.04.011

and physiological role (Nag et al., 2013a,b). RIO-1 (PFL1490w) and RIO-2 (PFD0975w), RIO like kinases are present in malaria kinome with uncharacterized functions (www.plasmodb.org). The structural characterization of RIO-2 kinase of *Plasmodium falciparum* (PfRIO-2 kinase) explored having *N*-terminal DNA binding winged helix domain, a linker region and C-terminal kinase domain together with well defined ATP binding pocket with significantly different than that of the human RIO-2 kinase (Trivedi and Nag, 2012).

It has been observed that natural products from plants and their synthetic, semi synthetic analogues are expected to play an imperative role in creating new and better chemotherapeutic agents. Artemisinin, a natural product and their semi-synthetic analogues are included in the first line treatment of malaria caused by dreadful species, *P. falciparum*. Another product from natural source was quinine which is another therapeutic approach in the treatment of malaria. Febrifugine, apigenin, and argentilactones are other natural products reported with high antimalarial activity (Koepfli et al., 1947; Carmona et al., 2003). Curcumin is a β-diketone obtained from the powdered root of *Curcuma longa Linn*., showed synergistic effect with artemisinin against *Plasmodium berghei* in vivo (Reddy et al., 2005; Nandakumar et al., 2006). It is also potent against both chloroquine susceptible and resistant strains of *P. falciparum* and exerted parasiticidal effect (Cui et al., 2007). Medicinal chemists have exploited four sites for chemical modification of curcumin, aryl side chain, diketo group, double bonds, and active methylene group and synthesized a number of curcumin analogues with improved biological activity. In the present investigation we report herein the modification of diketo group to pyrazole and pyrimidine heterocycles and their antimalarial activity. The molecular modelling approach was applied to these nineteen curcumin analogues to find the possible PfRIO2 kinase inhibitory action. Apart from molecular docking studies other possibilities such as optimized geometries, energies, spatial distribution, position of the highest occupied molecular orbital (HOMO) and the lowest unoccupied molecular orbital (LUMO), and quantitative structure activity relationship (QSAR) studies including structural and electronic properties could be applied to study the compounds' efficacy theoretically (Ibrahim and El-Haes, 2005; Ibrahim and Koglin, 2005; Hameed et al., 2007; Ess et al., 2008; Ibrahim et al., 2006, 2010, 2012; Saleh et al., 2014; Okasha et al., 2015). Various other biological activities, viz. anticancer (Ahsan et al., 2013; Liang et al., 2009; Jia et al., 2009), antibacterial (Lal et al., 2012; Sahu et al., 2012; Zhichang et al., 2012), anti-HIV (Singh et al., 2010), anti-inflammatory (Saja et al., 2007), antimalarial (Mishra et al., 2008), and many more have been reported for curcumin analogues. These recent developments made curcumin as an ideal lead compound for future drug discovery.

2. Results and discussion

2.1. Molecular modelling

The three dimensional structure of PfRIO2 kinase with four different binding sites namely S1–S4 was reported with several important active site residues. The ligand docking studies by choosing S1 and S2 sites of PfRIO2 have been studied earlier (Nag et al., 2013a,b; http://www.plasmodb.org; Parveen et al., 2013; Nag et al., 2013a). It might be due to closeness of S1 site with DNA binding site and S2 site with ATP. The S1 site was employed for the current ligand docking studies. The selected S1 site is comprised of the active site residues includes Trp26, Ser128, Lys131, Asp137, Leu141, His142, Tyr138, Lys135, Glu134, Val132, Arg136, Lys133, Thr127, Leu146, Arg149, Val145 and Ile148, and later it was found that is matching with earlier reported studies (Nag et al., 2013a,b; www.plasmodb.org; Parveen et al., 2013; Nag et al., 2013a) The S1 site is present at loop region which is flexible in nature. However, the present molecular docking studies of the curcumin analogues revealed that the binding mode is slightly different from earlier reported (Parveen et al., 2013). Due to higher molecular size and length of the curcumin analogues they occupied the selected active site (S1) totally. The overall major receptor interactions of all ligands observed were the $\pi - \pi$ interactions of His142 with one of the aromatic rings and sometimes along with aniline portion of the ligands. Val132 was the major residues that contributed its backbone with methoxy functional group present on the aromatic ring and Tyr26 exhibited the similar interactions with one or two ligands. π-Cationic interactions with Arg149 and Lys131 were found with the aniline part and pyrazole ring of the ligands. The Arg152 was present at another end of the ligands and was responsible for side chain H-bonding with methoxy functional group of aromatic ring repeatedly. The pyrazole bearing aromatic rings were observed to be present near to the DNA binding region of the protein. The docking studies finally suggested that the inhibitory activity of the current compounds may be due to interfering with normal functioning of the PfRIO2 kinase. The docking scores are given in the Table 1. The docking scores of the curcumin analogues reported herein showed more affinity towards PfRIO2 kinase than that of standard antimalarial drug chloroquine. The binding mode of all the ligands with the active site of PfRIO2 kinase is shown

Table 1 The glide score and E-model scores of the curcumin analogues (**3a–s**).

Compound	Glide score	E-model score
3a	−4.056	−59.44
3b	−4.043	−66.065
3c	−4.404	−60.514
3d	−4.763	−61.244
3e	−5.335	−65.602
3f	−5.289	−66.196
3g	−5.457	−61.647
3h	−5.861	−60.231
3i	−6.057	−66.997
3j	−5.236	−72.968
3k	−5.618	−76.206
3l	−5.442	−67.377
3m	−5.831	−61.797
3n	−5.486	−63.268
3o	−5.893	−74.414
3p	−4.213	−55.798
3q	−5.244	−60.119
3r	−5.719	−63.754
3s	−5.628	−66.947
Chloroquine	−4.959	−48.716

Please cite this article in press as: Balaji, S.N. et al., Molecular modelling, synthesis, and antimalarial potentials of curcumin analogues containing heterocyclic ring. Arabian Journal of Chemistry (2015), http://dx.doi.org/10.1016/j.arabjc.2015.04.011

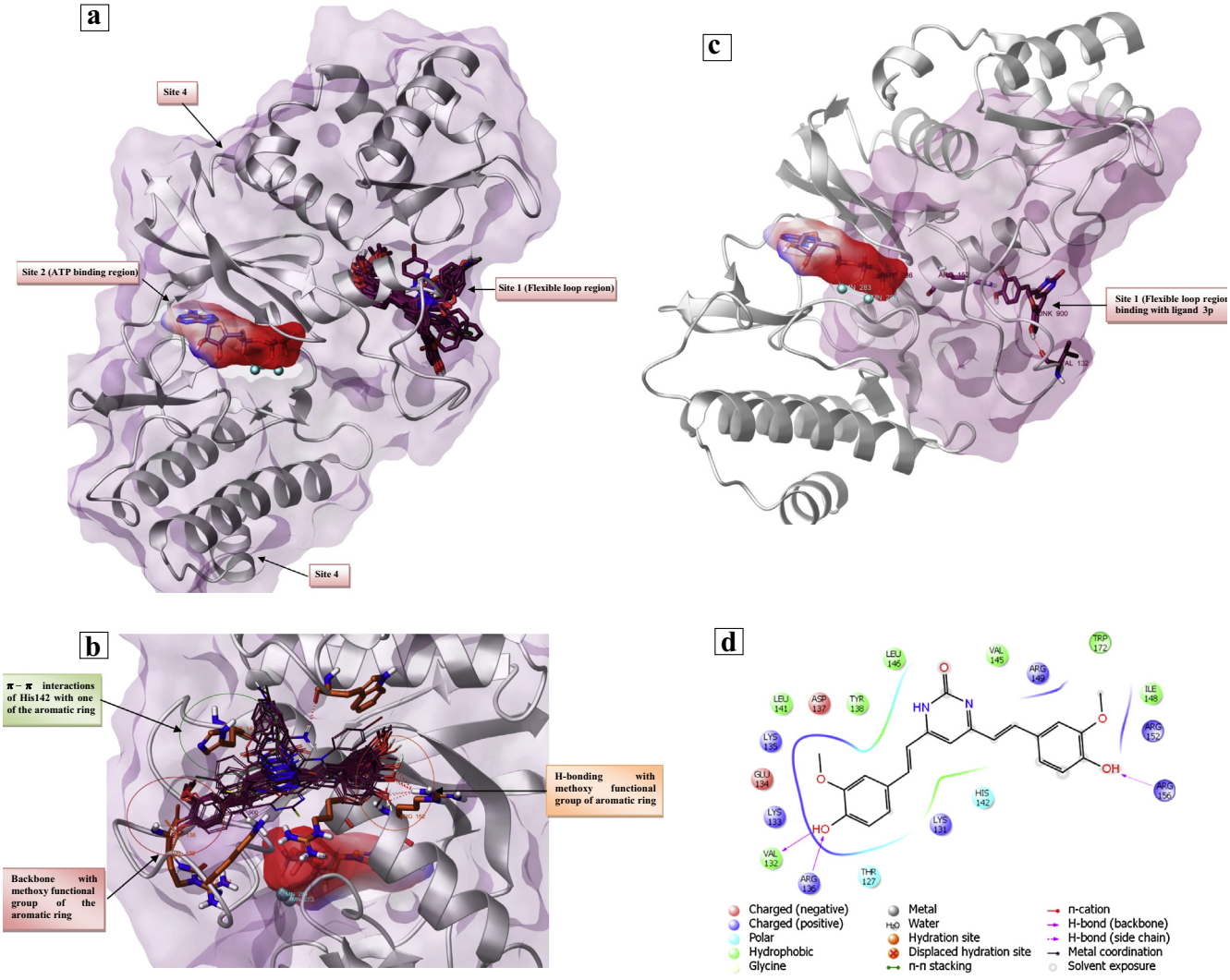

Figure 1 (a). PfRIO-2 kinase and various site and ligands (**3a–s**) binding at site 1 (S1). (b). The binding mode of all the ligands (**3a–s**) with the active site of PfRIO2 kinase and interactions. (c). The docking pose of ligand **3p** in the S1. (d). Ligand–receptor interaction diagram showing the major hot spot residues of S1 with compound **3p**.

in Fig. 1. The docking protocol can be validated using NMR would be an approach for the assessment of molecular recognition (Unione et al., 2014).

2.2. Chemistry

The curcumin analogues (**3a–s**) described in the study are shown in **Table 2** and the reaction sequence for the synthesis is summarized in **Scheme 1**. The synthesis of curcumin analogues was accomplished in four parts. 1,7-Bis(4-hydroxy-3-methoxyphenyl)hepta-1,6-diene-3,5-dione (curcumin, **1**) and substituted phenyl semicarbazide/hydrazide/urea/thiourea/ semicarbazide/thiosemicarbazide (**2a–s**) was refluxed in glacial acetic acid to obtain the 3,5-bis(4-hydroxy-3-methoxystyryl)-*N*-(substituted phenyl)-1H-pyrazole-1-carboxamide/ carbothioamide analogues (**3a–e**, **3r**, **3s**), 3,5-bis(4-hydroxy-3-methylstyryl)-1*H*-pyrazole-1-yl(substituted phenyl)methanone analogues (**3f–o**), and pyrimidine analogues (**3p–q**). We have reported the chemistry of 8 compounds earlier while 5 compounds were reported elsewhere (Ahsan et al., 2013; Lal et al., 2012; Sahu et al., 2012). In the present investigation we report herein 19 compounds including 6 new curcumin analogues.

2.3. Antimalarial activity

The schizonticidal and parasiticidal activity of synthetic curcumin analogues were determined as described previously (Parveen et al., 2013). The schizonticidal activity of the curcumin analogues showed IC_{50} of 1.48–23.09 μM. The compound **3a** showed maximum activity (IC_{50}; 9.87 ± 2.21 μM) among carboxamide analogues (**3a–e**). The compound **3l** showed maximum activity (IC_{50}; 4.21 ± 0.62 μM) among the methanone analogues (**3f–o**). The compound **3p** was found to be the most active compound with IC_{50} of 1.48 ± 0.10 μM, followed by the compound **3l** with IC_{50} of 4.21 ± 0.62 μM. The schizonticidal activity of the compounds (**3a–s**) is given in **Table 2**. The minimum killing concentration (MKC) was the concentration of the compounds required to kill the parasite present in the culture and is given in **Table 2**. The MKC of the compounds range between 3.87

Table 2 Antimalarial activity of curcumin analogues (**3a–s**).

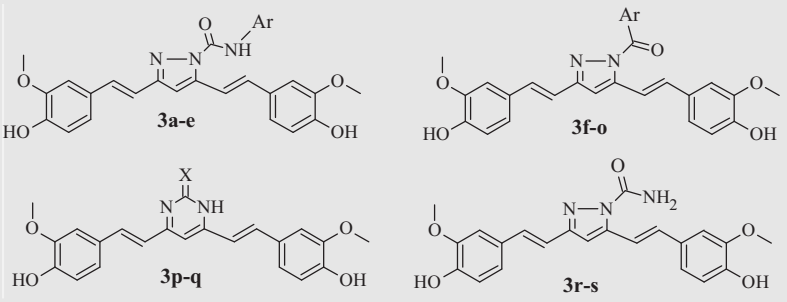

.

Compound	Ar//X	Schizonticidal Activity IC_{50} (μM ± SD)	Nature of inhibition	MKC (μM ± SD)
3a	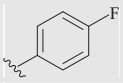	9.87 ± 2.21	parasiticidal	8.17 ± 0.78
3b	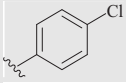	10.54 ± 0.67	parasiticidal	10.81 ± 1.41
3c	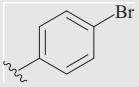	22.47 ± 1.72	parasiticidal	11.18 ± 2.11
3d	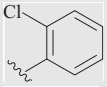	9.88 ± 0.11	parasiticidal	4.18 ± 0.08
3e	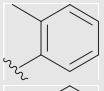	11.99 ± 1.62	parasiticidal	14.75 ± 0.06
3f	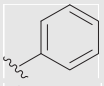	19.23 ± 0.34	parasiticidal	14.53 ± 2.05
3g	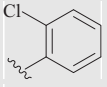	8.03 ± 0.26	parasiticidal	13.48 ± 0.0.73
3h	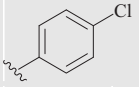	19.72 ± 2.05	parasiticidal	19.86 ± 0.66
3i	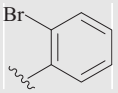	10.77 ± 2.26	parasiticidal	8.24 ± 0.27
3j	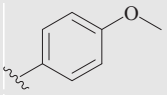	9.71 ± 0.14	parasiticidal	11.77 ± 0.22
3k	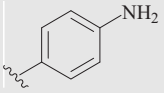	4.59 ± 0.16	parasiticidal	8.54 ± 0.06
3l	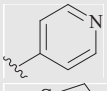	4.21 ± 0.62	parasiticidal	13.06 ± 0.04
3m	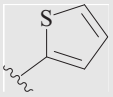	9.36 ± 0.53	parasiticidal	8.80 ± 1.41
3n	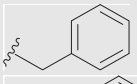	10.73 ± 1.66	parasiticidal	10.62 ± 0.19
3o	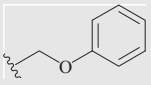	5.64 ± 0.72	parasiticidal	8.99 ± 0.90
3p	O	1.48 ± 0.10	parasiticidal	3.87 ± 0.36
3q	S	13.05 ± 3.03	parasiticidal	6.27 ± 0.09

Please cite this article in press as: Balaji, S.N. et al., Molecular modelling, synthesis, and antimalarial potentials of curcumin analogues containing heterocyclic ring. Arabian Journal of Chemistry (2015), http://dx.doi.org/10.1016/j.arabjc.2015.04.011

Table 2 (*continued*)

Compound	Ar//X	Schizonticidal Activity IC_{50} (μM ± SD)	Nature of inhibition	MKC (μM ± SD)
3r	O	12.17 ± 0.81	parasiticidal	25.35 ± 1.44
3s	S	23.09 ± 3.59	parasiticidal	24.70 ± 1.39
Chloroquine	–	0.078 ± 0.012[a]	–	–

A dash (–) indicates activity not done.
[a] Activity reported (Parveen et al., 2013).

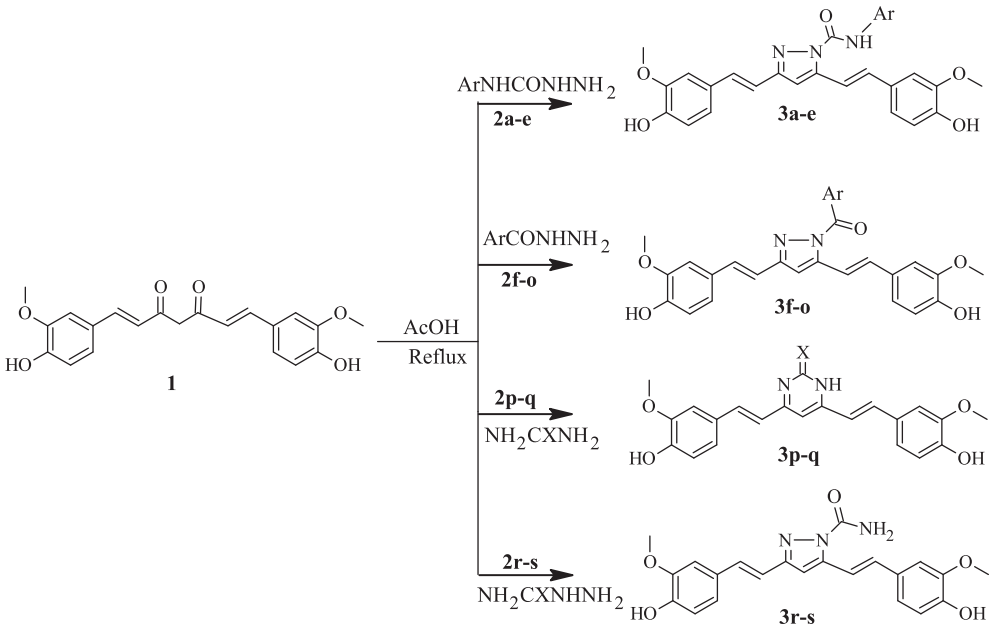

Scheme 1 Protocol for the synthesis of curcumin analogues (**3a–s**).

and 25.35 μM, and compound **3p** showed maximum activity with MKC of 3.87 ± 0.36 μM, followed by compound **3d** with MKC of 4.18 ± 0.08 μM. All the curcumin analogues (**3a–s**) showed parasiticidal activity. The structure activity relationship (SAR) was established with the antimalarial data showed that among carboxamide analogues (**3a–e**), 4-fluoro substitution is more favourable than 2-chloro, 4-chloro and 4-bromo, while 2-chloro substitution showed maximum MKC than 4-fluoro, 4-chloro and 4-bromo substitution in the aromatic ring. The antimalarial activity among methanone derivatives (**3f–o**) showed that substituted aromatic ring showed maximum activity than unsubstituted aromatic ring (**3f**, **3n**). The activity was maximum when 4-pyridyl ring (**3l**) was present followed by 4-amino (**3k**) substitution on aromatic ring. The curcumin analogues with pyrimidine/pyrazole with carbonyl function (**3p**, **3r**) showed maximum activity than thione function (**3q**, **3s**). The compound **3p** could be considered as promising lead for further optimization. Microscopic observation of infected RBCs exposed to synthetic curcumin compounds is shown in Fig. 2.

3. Experimental

3.1. Computational studies

The X-ray crystal structure of PfRIO-2 does not exist till date, the homology model using the RIO_2 of *Archaeoglobus fulgidus* (PDB: 1TQI) was reported few times (Nag et al., 2013a,b; http://www.plasmodb.org; Parveen et al., 2013; Nag et al., 2013a). The current experimental 3D-homology model was built using the sequences of PDBs 1ZAO (contains the ATP binding site and Mn ion) and AfRIO-2 by employing Prime module (Nag et al., 2013a,b; http://www.plasmodb.org; Parveen et al., 2013; Nag et al., 2013a). The natural bound ligand along with Mn ion placed at functional site of the 3D model by superimposition of model and $AfRIO_2$ co-crystal complex. The final model was then prepared with all necessary parameters using the protein preparation wizard with default parameters. The experimental model contains the metal ions (divalent) and ATP complex. All the chemical structures of the ligands were drawn using the ACD chemsketch and saved as mol. files and imported in Maestro and prepared by using the Ligprep. Further XP protocol implemented in Glide was employed for the ligand docking studies. The homology model developed must be validated for its quality; the current model was validated using the online server RAMPAGE, it gives the quality of the structure. The Ramachandran plot of current model exhibited that, 93.2% of the residues were present in the favoured region, 5.0% were in allowed region and 1.8% in outlier region. The available co-crystal structures of the RIO-2 exhibited the binding site of the ATP along with Mn ions only, we adopted the sitemap analysis tool of the Schrodinger LLC in order identify the possible binding site. The possible four various binding regions were identified

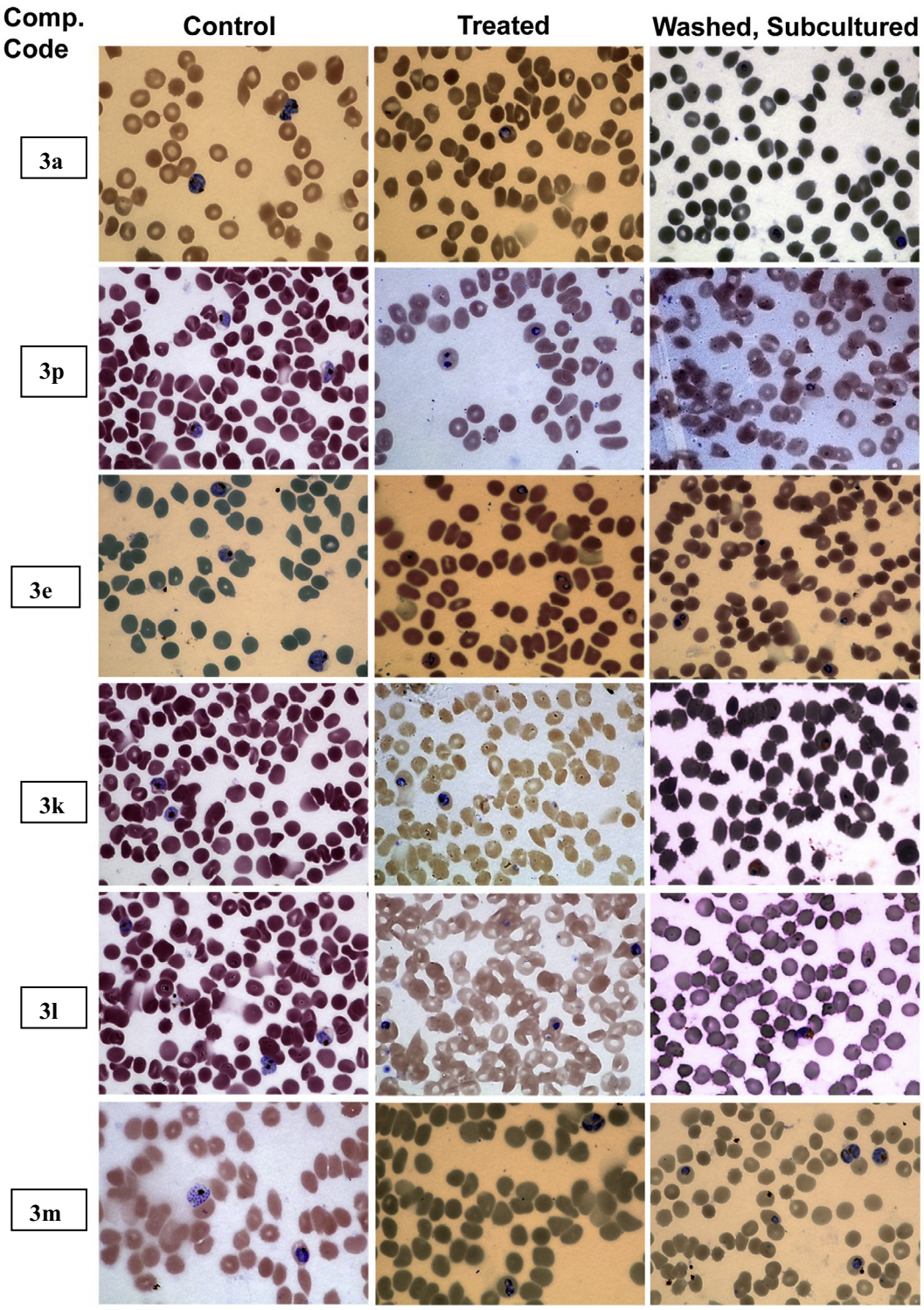

Figure 2 Microscopic observation of infected RBCs exposed to synthetic curcumin compounds. The parasite in the untreated condition (“Control”) is exhibiting healthy parasite with different blood stages. The parasite in the treated condition (“Treated”) is either halting at ring stage or giving dead parasites. Washing with complete media to remove compounds (“Washed, sub-culture”) and sub-culturing of parasite indicate that most of the compounds are parasiticidal with no infected cells or dead parasites (parasite without cell membrane).

through it. Among them the flexible loop regions was selected for further processes (Nag et al., 2013a,b; www.plasmodb.org; Parveen et al., 2013; Nag et al., 2013a). The selected site was employed for the receptor grid generation (Fig. 1a and b).

3.2. Chemistry

All chemicals were supplied by E. Merck (Germany), Konark Herbal (India) and S. D. Fine Chemicals (India). Melting

points were determined by open tube capillary method and are uncorrected. Purity of the compounds was checked by elemental analysis and the progress of reactions was monitored by TLC plates (silica gel G) using mobile phase, hexane: ethylacetate (6:4), and the spots were identified by iodine vapours or UV light. IR spectra were obtained on a Schimadzu 8201 PC, FT-IR spectrometer (KBr pellets). ^{1}H NMR spectra were recorded on a Bruker AC 300/400 MHz spectrometer using TMS as internal standard in DMSO. Mass spectra were recorded on a Bruker Esquire LCMS using ESI and elemental analyses were performed on Perkin–Elmer 2400 Elemental Analyzer.

*3.3. General method for the synthesis of 3,5-bis(4-hydroxy-3-methylstyryl)-N-(substituted phenyl)-1H-pyrazole-1-carboxamide analogues (**3a–e**)*

1,7-Bis(4-hydroxy-3-methoxyphenyl)hepta-1,6-diene-3,5-dione (**1**) (0.005 mol) and substituted phenyl semicarbazide (**2a–e**) (0.005 mol) were refluxed in glacial acetic acid for 12 h (Ahsan et al., 2013). The excess of solvent was removed under reduced pressure and then the reaction mixture was poured into the crushed ice. The solid mass was filtered, washed, dried and recrystallized with ethanol furnished the title 3,5-bis(4-hydroxy-3-methylstyryl)-*N*-(substitutedphenyl)-1*H*-pyrazole-1-carboxamide analogues (**3a-e**).

*3.3.1. 3,5-Bis(4-hydroxy-3-methylstyryl)-N-(4-fluorophenyl)-1H-pyrazole-1-carboxamide (**3a**)*

M.p. 70 °C; yield 72% (Ahsan et al., 2013).

*3.3.2. 3,5-Bis(4-hydroxy-3-methylstyryl)-N-(4-chlorophenyl)-1H-pyrazole-1-carboxamide (**3b**)*

M.p. 78 °C; yield 66% (Ahsan et al., 2013).

*3.3.3. 3,5-Bis(4-hydroxy-3-methylstyryl)-N-(4-bromophenyl)-1H-pyrazole-1-carboxamide (**3c**)*

M.p. 136 °C; yield 74% (Ahsan et al., 2013).

*3.3.4. 3,5-Bis(4-hydroxy-3-methylstyryl)-N-(2-chlorophenyl)-1H-pyrazole-1-carboxamide (**3d**)*

M.p. 92 °C; yield 76% (Ahsan et al., 2013).

*3.3.5. 3,5-Bis(4-hydroxy-3-methylstyryl)-N-(2-methylphenyl)-1H-pyrazole-1-carboxamide (**3e**)*

M.p. 98 °C; yield 7% (Ahsan et al., 2013).

*3.4. General method for the synthesis of 3,5-bis(4-hydroxy-3-methylstyryl)-1H-pyrazole-1-yl(substituted phenyl)methanone analogues (**3f–o**)*

1,7-Bis(4-hydroxy-3-methoxyphenyl)hepta-1,6-diene-3,5-dione (**1**) (0.005 mol) and substituted phenyl hydrazide (**2f–o**) (0.005 mol) were refluxed in glacial acetic acid for 12 h. The excess of solvent was removed under reduced pressure and then the reaction mixture was poured into the crushed ice. The solid mass was filtered, washed, dried and recrystallized with ethanol furnished the title 3,5-bis(4-hydroxy-3-methylstyryl)-1*H*-pyrazole-1yl(substituted phenyl)methanone analogues (**3f–o**) (Ahsan et al., 2013).

*3.4.1. 3,5-Bis(4-hydroxy-3-methoxystyryl)-1H-pyrazole-1-yl(phenyl)methanone (**3f**)*

M.p. 110 °C; yield 84% (Ahsan et al., 2013).

*3.4.2. 3,5-Bis(4-hydroxy-3-methylstyryl)-1H-pyrazole-1-yl-(2-chlorophenyl)methanone (**3g**)*

M.p. 168–170 °C; yield 74%; IR (KBr) cm^{-1}: 3412 (OH), 1751 (C═O), 1569 (C═N), 1329 (C—N), 699 (C—Cl). ^{1}H NMR (400 MHz, DMSO-d_6): δ 3.83 (6H, s, OCH_3), 6.61 (1H, s, CH═C), 6.76 (2H, d, J = 12.1 Hz, CH and CH), 6.90 (2H, d, J = 12.1 Hz, CH and CH), 6.94–8.17 (10H, m, ArH), 9.15 (2H, s, OH); m/z = 503.0 (M^+). Cal/Ana: [C (66.85) 66.87 H (4.63) 4.61 N (5.55) 5.57].

*3.4.3. 3,5-Bis(4-hydroxy-3-methylstyryl)-1H-pyrazole-1-yl-(4-chlorophenyl)methanone (**3h**)*

M.p. 160–162 °C; yield 78%; IR (KBr) cm^{-1}: 3406 (OH), 1745 (C═O), 1562 (C═N), 1337 (C—N), 698 (C—Cl). ^{1}H NMR (400 MHz, DMSO-d_6): δ 3.83 (6H, s, OCH_3), 6.61 (1H, s, CH═C), 6.75 (2H, d, J = 11.6 Hz, CH and CH), 6.91 (2H, d, J = 11.6 Hz, CH and CH), 6.93–7.89 (10H, m, ArH), 9.14 (2H, s, OH), 9.89 (1H, s, OH); m/z = 503.0 (M^+). Cal/Ana: [C (66.84) 66.87 H (4.63) 4.61 N (5.54) 5.57].

*3.4.4. 3,5-Bis(4-hydroxy-3-methoxystyryl)-1H-pyrazole-1-yl(2-bromophenyl)methanone (**3i**)*

M.p. 288 °C; yield 76% (Ahsan et al., 2013).

*3.4.5. 3,5-Bis(4-hydroxy-3-methylstyryl)-1H-pyrazole-1-yl-(4-methoxyphenyl)methanone (**3j**)*

M.p. 128–130 °C; yield 74%; IR (KBr) cm^{-1}: 3407 (OH), 1745 (C═O), 1561 (C═N), 1334 (C—N), 745 (C—Cl). ^{1}H NMR (400 MHz, DMSO-d_6): δ 3.83 (9H, s, OCH_3), 6.61 (1H, s, CH═C), 6.76 (2H, d, J = 12.2 Hz, CH and CH), 6.92 (2H, d, J = 12.2 Hz, CH and CH), 6.92–7.92 (10H, m, ArH), 9.15 (1H, s, OH), 10.28 (1H, s, OH). ^{13}C NMR (100 MHz, DMSO-d_6): δ 55.9, 56.2, 107.7, 112.0, 114.8, 116.8, 120.1, 122.9, 123.6, 128.8, 130.9, 133.4, 133.9, 144.9, 147.3, 151.3, 165.1, 166.5; m/z = 499.1 (M^+). Cal/Ana: [C (69.85) 69.87 H (5.24) 5.26 N (5.65) 5.62].

*3.4.6. 3,5-Bis(4-hydroxy-3-methylstyryl)-1H-pyrazole-1-yl-(4-aminophenyl)methanone (**3k**)*

M.p. 215–217 °C (reported), 212–214 °C (found); yield 71% (Sahu et al., 2012).

*3.4.7. 3,5-Bis(4-hydroxy-3-methylstyryl)-1H-pyrazole-1-yl-(pyrid-4-yl)methanone (**3l**)*

M.p. 105–106 °C(reported), 104–106 °C (found); yield 71% (Sahu et al., 2012).

*3.4.8. 3,5-Bis(4-hydroxy-3-methylstyryl)-1H-pyrazole-1-yl-(2-thiophenyl)methanone (**3m**)*

M.p. 120–122 °C; yield 65%; IR (KBr) cm^{-1}: 3396 (OH), 1735 (C═O), 1563 (C═N), 1337 (C—N). ^{1}H NMR (400 MHz, DMSO-d_6): δ 3.83 (6H, s, OCH_3), 6.61 (1H, s, CH═C), 6.76 (2H, d, J = 12.8 Hz, CH and CH), 6.89 (2H, d, J = 12.8 Hz, CH and CH), 6.92–7.88 (9H, m, ArH), 10.53 (2H, s, OH);

m/z = 475.1 (M^+). Cal/Ana: [C (65.84) 65.81 H (4.65) 4.67 N (5.94) 5.90].

*3.4.9. 3,5-Bis(4-hydroxy-3-methylstyryl)-1H-pyrazole-1-yl-(phenyl)ethanone (**3n**)*

M.p. 138–140 °C; yield 82%; IR (KBr) cm^{-1}: 3401 (OH), 1751 (C═O), 1565 (C═N), 1338 (C─N). ^1H NMR (400 MHz, DMSO-d_6): δ 3.66 (2H, s, CH_2), 3.83 (6H, s, OCH_3), 6.61 (1H, s, CH═C), 6.76 (2H, d, *J* = 11.8 Hz, CH and CH), 6.89 (2H, d, *J* = 11.8 Hz, CH and CH), 6.94–7.81 (11H, m, ArH), 9.15 (2H, s, OH); *m/z* = 482.6 (M^+). Cal/Ana: [C (72.14) 72.18 H (5.47) 5.43 N (5.79) 5.81].

*3.4.10. 3,5-Bis(4-hydroxy-3-methylstyryl)-1H-pyrazole-1-yl-(phenoxyl)methanone (**3o**)*

M.p. 130–132 °C; yield 76%; IR (KBr) cm^{-1}: 3402 (OH), 1755 (C═O), 1569 (C═N), 1334 (C─N), 745 (C─Cl). ^1H NMR (400 MHz, DMSO-d_6): δ 3.79 (2H, s, OCH_2), 3.83 (6H, s, OCH_3), 6.61 (1H, s, CH═C), 6.76 (2H, d, *J* = 11.8 Hz, CH and CH), 6.90 (2H, d, *J* = 11.8 Hz, CH and CH), 6.94–7.38 (10H, m, ArH), 9.15 (2H, s, OH); *m/z* = 499.1 (M^+). Cal/Ana: [C (69.84) 69.87 H (5.25) 5.26 N (5.64) 5.62].

*3.5. General method for the synthesis of dihydropyrimidine analogues (**3p** and **3q**)*

1,7-Bis(4-hydroxy-3-methoxyphenyl)hepta-1,6-diene-3,5-dione (**1**) (0.005 mol) and urea/thiourea (**2p–q**) (0.005 mol) were refluxed in glacial acetic acid for 12 h. The excess of solvent was removed under reduced pressure and then the reaction mixture was poured into the crushed ice. The solid mass was filtered, washed, dried and recrystallized with ethanol furnished the title 3,5-bis(4-hydroxy-3-methylstyryl)-*N*-(substitutedphenyl)-1*H*-pyrazole-1-carboxamide analogues (**3p–q**) (Ahsan et al., 2013).

*3.5.1. 4,6-Bis(4-hydroxy-3-methoxystyryl)pyrimidine-2(1H)-one (**3p**)*

M.p. 104 °C; yield 72% (Ahsan et al., 2013).

*3.5.2. 4,6-Bis(4-hydroxy-3-methoxystyryl)pyrimidine-2(1H)-thione (**3q**)*

M.p. 102–104 °C; yield 75% (Ahsan et al., 2013).

*3.6. General method for the synthesis of 3,5-bis(4-hydroxy-3-methylstyryl)-1H-pyrazole-1-carboxamide/carbothiamide analogues (**3r** and **3s**)*

1,7-Bis(4-hydroxy-3-methoxyphenyl)hepta-1,6-diene-3,5-dione (**1**) (0.005 mol) and semicarbazide/thiosemicarbazide (**2r–s**) (0.005 mol) were refluxed in glacial acetic acid (AcOH) for 12 h. The progress of reaction was monitored throughout by TLC plates (silica gel G) using mobile phase, hexane: ethylacetate (6:4), and the spots were identified by iodine vapours or UV light. The excess of solvent was removed under reduced pressure and then the reaction mixture was then poured into the crushed ice. The solid mass was filtered, washed, dried and recrystallized with ethanol furnished the title of 3,5-bis(4-hydroxy-3-methylstyryl)-1*H*-pyrazole-1-carboxamide/carbothioamide analogues (**3r** and **3s**).

*3.6.1. 3,5-Bis(4-hydroxy-3-methylstyryl)-1H-pyrazole-1-carboxamide (**3r**)*

M.p. 204–206 °C (reported), 200–202 °C (found); yield 84% (Lal et al., 2012).

*3.6.2. 3,5-Bis(4-hydroxy-3-methylstyryl)-1H-pyrazole-1-carboxamide (**3s**)*

M.p. 100–101 °C (reported), 102 °C (found); yield 79% (Lal et al., 2012).

3.7. Antimalarial activity

The schizonticidal and parasiticidal activity of synthetic curcumin analogues were determined as described previously (Parveen et al., 2013). In brief, parasite culture was treated with D-sorbitol and then ring stage parasite incubated with different concentration of test compounds. After 42 h incubation, smear was prepared and stained with Giemsa stain to monitor the maturation of ring stage parasites into schizonts. To determine the nature of parasite growth inhibition (parasitostatic/parasiticidal), the compounds were removed and the cultures were washed three times with albumax II free RPMI-1640 and incubated in complete media with fresh haematocrit for another 72 h. A thin smear was prepared, and number of RBCs containing viable parasite was counted. The minimum concentration of compounds giving no viable parasite was used to calculate minimum killing concentration (MKC) of compounds with parasiticidal activity.

4. Conclusion

All the compounds were synthesized in satisfactory yield. The molecular modelling studies revealed that the curcumin analogues completely occupied the S1 site of PfRIO-2 kinase with different binding modes. All the synthesized compounds showed significant antimalarial activity with parasiticidal nature. One of the synthesized compounds (**3p**) with significant results was identified as promising lead for further studies and drug discovery in the field of malaria therapeutics. The detailed studies to acquire more information are in progress in our laboratories.

Acknowledgments

The management of Maharishi Arvind College of Pharmacy, Jaipur, Rajasthan, India is acknowledged for providing research facilities. The authors are thankful to Dr. Reddy Life Science, Hyderabad, India for spectral analysis. This work was partially supported by the Department of Biotechnology; Govt of India Grants (BT/PR13436/MED/12/450/2009 & BT/41/NE/TBP/2010) to V.T. SNB acknowledges the institute fellowship from Indian Institute of Technology-Guwahati, Assam, India to carry out this work.

References

Ahsan, M.J., Khalilullah, H., Yasmin, S., Jadav, S.S., Govindasamy, J., 2013. Synthesis, characterisation, and in vitro anticancer activity of curcumin analogues bearing pyrazole/pyrimidine Ring targeting EGFR tyrosine kinase. BioMed Res. Int. 2013, 1–14. http://dx.doi.org/10.1155/2013/239354.

Carmona, D., Saez, J., Granados, H., Perez, E., Blair, S., Angulo, A., Figadere, B., 2003. Antiprotozoal 6-substituted-5,6-dihydro-alpha-pyrones from *Raimondia cf. monoica*. Nat. Prod. Res. 17, 275–280.

Cui, L., Miao, J., Cui, L., 2007. Cytotoxic effect of curcumin on malaria parasite *Plasmodium falciparum*: inhibition of histone acetylation and generation of reactive oxygen species. J. Antimicrob. Agents Chemother. 51, 488–494.

Essa, A.H., Ibrahim, M., Hameed, A.J., Al-Masoudi, N.A., 2008. Theoretical investigation of 3'-subtituted-2'-3'-dideoxythymidines related to AZT. QSAR infrared and substituent electronic effect studies. ARKIVOC (xiii) 255–265.

Hameed, A.J., Ibrahim, M., ElHaes, H., 2007. Computational notes on structural, electronic and QSAR properties of Fulleropyrrolidine-1-carbodithioic acid 2; 3 and 4-substituted-benzyl esters. J. Mol. Struct THEOCHEM. 809, 131–136.

Ibrahim, M., El-Haes, H., 2005. Computational spectroscopic study of copper, cadmium, lead and zinc interactions in the environment. Int. J. Environ. Pollut. 23, 417–424.

Ibrahim, M., Koglin, E., 2005. Spectroscopic study of polyaniline emeraldine base: modelling approach. Acta Chim. Slov. 52, 159–163.

Ibrahim, M., Alaam, M., El-Haes, H., Jalbout, A.F., deLeon, A., 2006. Analysis of the structure and vibrational spectra of glucose and fructose. Ecl. Quim. Sao Paulo 31, 15–21.

Ibrahim, M., Saleh, N.A., Hameed, A.J., Elshemey, W.M., Elsayed, A.A., 2010. Structural and electronic properties of new fullerene derivatives and their possible application as HIV-1 protease inhibitors. Spectrochim. Acta Part A 75, 702–709.

Ibrahim, M., Saleh, N.A., Elshemey, W.M., Elsayed, A.A., 2012. Fullerene derivative as anti-HIV protease inhibitor: molecular modeling and QSAR approaches. Mini Rev. Med. Chem. 12, 447–451.

Jia, Y., Li, J., Qin, Z.H., Liang, Z.Q., 2009. Autophagic and apoptotic mechanisms of curcumin-induced death in K562 cells. J. Asian Nat. Prod. Res. 11, 918–928.

Koepfli, J.B., Mead, J.F., Brockman, J.A., 1947. An alkaloid with high antimalarial activity from Dichroa Febrifuga1. J. Am. Chem. Soc. 69, 1837-1837.

Kumar, S., Bandyopadhyay, U., 2005. Free heme toxicity and its detoxification systems in human. Toxicol. Lett. 157, 175–188.

Lal, J., Gupta, S.K., Thavaselvam, D., Agrawal, D.D., 2012. Design, synthesis, synergistic antimicrobial activity and cytotoxicity of 4-aryl substituted 3,4-dihydropyrimidinones of curcumin. Bioorg. Med. Chem. 22, 2872–2876.

Liang, G., Shao, L., Wang, Y., Zhao, C., Chu, Y., Xiao, J., Zhao, Y., Li, X., Yang, S., 2009. Exploration and synthesis of curcumin analogues with improved structural stability both in vitro and in vivo as cytotoxic agents. Bioorg. Med. Chem. 17, 2623–2631.

Mishra, S., Karmodiya, K., Surolia, N., Surolia, A., 2008. Synthesis and exploration of novel curcumin analogues as anti-malarial agents. Bioorg. Med. Chem. 16, 2894–2902.

Nag, S., Chouhan, D.K., Balaji, S.N., Chakraborty, A., Lhouvum, K., Bal, C., Sharon, A., Trivedi, V., 2013a. Comprehensive screening of hetrocyclic compound librararies, to identify novel inhibitors for PfRIO2 kinase through docking and substrate competition studies. Med. Chem. Res. 22, 4737.

Nag, S., Prasad, K., Bhowmick, A., Deshmukh, R., Trivedi, V., 2013b. PfRIO-2 kinase is a potential therapeutic target of antimalarial protein kinase. Curr. Drug Dis. Tech. 10, 85–91.

Nandakumar, D.N., Nagaraj, V.A., Vathsala, P.G., Rangarajan, P., Padmanaban, G.J., 2006. Curcumin-artemisinin combination therapy for malaria. Antimicrob. Agents Chemother. 50, 1859–1860.

Okasha, A., Gomaa, F., Elhaes, H., Morsey, M., El-Khodary, S., Fakhry, A., Ibrahim, M., 2015. Spectroscopic analyses of the photocatalytic behavior of nano titanium dioxide. Spectrochim. Acta A 136, 504–509.

Parveen, A., Chakraborty, A., Konreddy, A.K., Chakravarty, H., Sharon, A., Trivedi, V., Bal, C., 2013. Skeletal hybridization and PfRIO-2 kinase modeling for synthesis of α-pyrone analogs as anti-malarial agent. Eur. J. Med. Chem. 70, 607–612.

Phyo, A.P., Nkhoma, S., Stepniewska, K., Ashley, E.A., Nair, S., McGready, R., Al-Saai, S., Dondorp, A.M., Lwin, K.M., Singhasivanon, P., 2012. Emergence of artemisininresistant malaria on the western border of Thailand: a longitudinal study. Lancet 379, 1960–1966.

Reddy, R.C., Vatsalab, P.G., Keshamounia, V.G., Padmanaban, G., Rangarajan, P.N., 2005. Biochem. Curcumin for malaria therapy. Biophys. Res. Commun. 326, 472–474.

Sahu, P.K., Sahu, P.K., Gupta, S.K., Thavaselvam, D., Agarwal, D.D., 2012. Synthesis and evaluation of antimicrobial activity of 4H-pyrimido[2,1-b]benzothiazole, pyrazole and benzylidene derivatives of curcumin. Eur. J. Med. Chem. 54, 366–378.

Saja, K., Babu, M.S., Karunagaran, D., Sudhakaran, P.R., 2007. Anti-inflammatory effect of curcumin involves downregulation of MMP-9 in blood mononuclear cells. Int. Immunopharm. 7, 1659–1667.

Saleh, N.A., Elfiky, A.A., Ezat, A.A., Elshemey, W.M., Ibrahim, M., 2014. The electronic and QSAR properties of modified telaprevir compounds as HCV NS3 protease inhibitors. J. Comput. Theor. Nanosci. 11, 544–548.

Singh, R.K., Rai, D., Yadav, D., Bhargava, A., Balzarini, J., DeClercq, E., 2010. Synthesis, antibacterial and antiviral properties of curcumin bioconjugates bearing dipeptide, fatty acids and folic acid. Eur. J. Med. Chem. 45, 1078–1086.

Trivedi, V., Nag, S., 2012. In silico characterization of atypical kinase PFD0975w from plasmodium kinome: a suitable target for drug discovery. Chem. Biol. Drug Des. 79, 600–609.

Unione, L., Galanta, S., Diaz, D., Canada, F.J., Jimenez-Barbero, J., 2014. NMR and molecular recognition. The application of ligand-based NMR methods to monitor molecular interactions. Med. Chem. Commun. 5, 1280–1289.

WHO World malaria report 2013. ISBN 9789241564694. <http://www.plasmodb.org> (accessed 25.06.14).

Zhichang, L., Yinghong, W., Yuanqin, Z., Qinxiang, X., 2012. Synthesis and antibacterial activities of *N*-Substituted pyrazole curcumin derivatives. Chin. J. Org. Chem. 32, 1487–1492.

Please cite this article in press as: Balaji, S.N. et al., Molecular modelling, synthesis, and antimalarial potentials of curcumin analogues containing heterocyclic ring. Arabian Journal of Chemistry (2015), http://dx.doi.org/10.1016/j.arabjc.2015.04.011